Sensors and Materials, Vol. 34, No. 7 (2022) 2735–2745
MYU Tokyo

S & M 3002

Carbon-nanotube-based Gas Preconcentration for Breath Analysis

Keiji Nakamoto, Tomoaki Kageyama, Shunsaku Hosoi,
Tadao Matsunaga, and Sang-Seok Lee*

Graduate School of Engineering, Tottori University, 4-101 Koyama-Minami, Tottori 680-8552, Japan

(Received April 30, 2022; accepted June 28, 2022)

Keywords: carbon nanotube, micro-preconcentrator, VOC gas sensing, breath analysis

This paper presents a volatile organic compound (VOC) gas preconcentration method based on microstructures. The microstructures have a flower-leaf-type pattern, and each microstructure consists of carbon nanotubes (CNTs). This pattern is optimized by performing a simulation study to maximize the adsorption area between the VOC gas flow and the microstructure surfaces. The VOC gases contained in the exhaled breath of a human or dog can be utilized as biomarkers of cancers. Therefore, trace-level VOC gas detection in exhaled breath can enable the early diagnosis of human or canine cancer. We propose a method for analyzing human or canine breath using CNT-based gas preconcentration and conventional gas sensors or gas analysis equipment. To validate the method, we fabricated a CNT-based micro-preconcentrator and experimentally investigated ppb-level gas adsorption and detection with conventional gas chromatography equipment. As a result, we achieved more than 1000-fold gas preconcentration and ppb-level gas detection using conventional gas chromatography, which can normally only detect ppm-level gases.

1. Introduction

Globally, cancer is the second leading cause of death behind cardiovascular disease,[1,2] and since 1981, the leading cause of death in Japan has been cancer.[3] However, the death rate due to cancer is decreasing gradually because of the development of cancer treatments and early cancer diagnosis methods.

Many researchers of sensors and MEMS have conducted studies to diagnose cancer earlier, more rapidly, and more accurately. Among these studies, in this study, we focus on early cancer diagnosis methods based on microscale devices, because early cancer diagnosis is the most important factor in reducing mortality.[4] Most microscale devices used for early cancer diagnosis are microfluidic devices. These devices are mainly used for blood testing and were developed to detect circulating tumor cells or cell-free circulation tumor DNA in the blood (as examples, see Refs. 5 and 6). In addition to microfluidic-device-based cancer diagnosis, a saliva test method[7] and a test using nematode (*Caenorhabditis elegans*) olfaction[8] have been proposed for early cancer diagnoses. Although both tests are simple and cheap, they have

*Corresponding author: e-mail: sslee@tottori-u.ac.jp
https://doi.org/10.18494/SAM3965

ISSN 0914-4935 © MYU K.K.

disadvantages. For the saliva test, it takes two weeks to obtain the result, and the saliva must be taken from a person at rest. For the method using nematode olfaction, we cannot specify the cancer because it uses the characteristic of the nematode that it moves to the urine of a cancer patient.

As another simple, cheap, and breakthrough cancer diagnosis method, breath analysis is currently a strong focus of research. Cancer diagnosis based on breath analysis has many advantages: no pain, no use of radioactivity, low cost, quantitative diagnosis, and the ability to diagnose various cancers simultaneously.[9–13] In the medical field, a preconcentrator tube[9] or a gas sampling bag[14] such as a Tedlar bag has been used to capture exhaled breath for breath analysis. However, a preconcentrator tube is not handheld device because of its large size. Furthermore, trace-level gas detection using a preconcentrator is difficult because its preconcentration capability is limited. Another difficulty in the analysis of captured gases is that the sensitivity of conventional gas sensors or gas component analysis equipment is insufficient to detect less than ppm-order trace-level volatile organic compound (VOC) gases.

To use breath analysis as an early and more convenient cancer diagnosis method, two problems must be solved: to improve the preconcentrator capability and the sensitivity of gas sensors or gas component analysis equipment. To overcome these problems, many researchers have been striving to develop sensors with high sensitivity. Conversely, a few researchers have been trying to develop smaller preconcentrators and preconcentrators with higher preconcentration capability. Sensors for application to breath analysis have been proposed by several groups.[15–17] However, the sensors are still large and not portable, or the sensitivity has not yet reached ppb order. Regarding research on preconcentrators, the preconcentration capability has been improved by the application of MEMS technology, and the device size has also been reduced to the microscale. With a MEMS-based micro-preconcentrator, ppb-level VOC gas detection was demonstrated experimentally.[18] In the experiment, ppb-level VOC mixture gases were preconcentrated by being adsorbed onto Si microstructures in a micro-preconcentrator. Then, the preconcentrated gases were desorbed and introduced into a gas chromatography device for gas analysis. As a result, ppb-level VOC mixture gases were successfully detected by conventional gas chromatography, whose detectable gas concentration limit is ppm order.

The breath analysis method has the many advantages mentioned above as an early cancer diagnosis method, and micro-preconcentrator-based breath analysis appears to be a more promising approach than sensor-based breath analysis. In the case of micro-preconcentrator-based breath analysis, gas components can be analyzed by conventional gas component analysis equipment such as gas chromatography or gas mass chromatography equipment, which is an advantage over developing sensors for breath analysis. There are many VOC gas biomarker candidates for each cancer. For example, in the case of breast cancer, biomarker candidates are classified into ten groups, each consisting of three VOC gases.[9] Therefore, it is difficult to develop sensors to simultaneously detect many biomarker candidates.

We have proposed a MEMS-based micro-preconcentrator for application to cancer diagnosis that consists of flower-leaf-shaped Si microstructures.[19] These microstructures were designed through a quantitative simulation model to improve the micro-preconcentrator capability. In this

study, we present a micro-preconcentrator in which the microstructures used to capture VOC gases consist of carbon nanotubes (CNTs), which lead to better preconcentration capability than that of a Si-based micro-preconcentrator. We applied the flower leaf shape to the microstructure pattern. We conducted a simulation study to confirm the gas adsorption capability of the microstructures consisting of CNTs. Moreover, we fabricated a CNT-based micro-preconcentrator and conducted an experiment with ppb-level VOC gases to demonstrate its preconcentration capability. The design and fabrication of the micro-preconcentrator and the experimental results of ppb-level VOC gas detection are presented in the following sections.

2. Simulation Study on Gas Adsorption Capability of CNTs

In the case of MEMS-based micro-preconcentrators, the larger the surface area of the microstructures, the greater the adsorption capability. However, without considering the fluid flow during the design process, the effect of increasing the microstructure surface area will be less than expected.[18] In a previous study, we designed the microstructure by considering the fluid flow.[19] In other words, to maximize the contact surface between the fluid flow and the microstructure surfaces, we designed the shape of the microstructure using a quantitative finite element method (FEM) simulation model. In the simulation, we considered Si as the microstructure material and investigated the effect of the design parameters, such as the microstructure pattern shape, microstructure pattern size, microstructure array configuration, chamber shape, and the numbers of inlets and outlets. The adsorption capability was evaluated by counting the number of gas molecules reaching the 3D Si microstructure surface. Details of the simulation models and results for the 3D Si microstructures will be presented elsewhere. Here, we only mention that flower-leaf-shaped microstructures with a staggered configuration were found to have the greatest adsorption capability; these microstructures are illustrated in Fig. 1 along with their dimensions.

We conducted a simulation study to determine the adsorption capability of a microstructure consisting of a CNT forest. The flower leaf shape mentioned above was used for the CNT forest pattern. In the simulation model, the flower-leaf-shaped Si microstructure was replaced with a CNT forest as shown in Fig. 2. The flower-leaf-shaped pattern was filled with 100-nm-diameter CNT bundles with a distance of 100 nm between the bundles. We were unable to simulate a full-

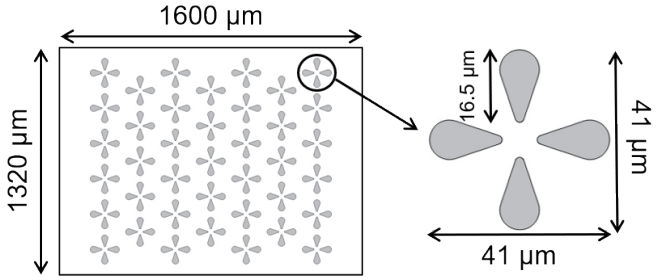

Fig. 1. Top view of simulation model: this model shows the greatest adsorption capability among the investigated Si-based models. Flower-leaf-shaped microstructures with a staggered configuration were found to exhibit the greatest adsorption capability.

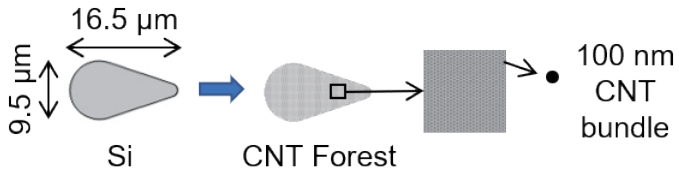

Fig. 2. (Color online) CNT forest used to replace Si microstructure model to investigate adsorption capability of micro-preconcentrator consisting of CNTs. The CNT forest was filled with 100-nm-diameter CNT bundles with a distance of 100 nm between the bundles.

scale 3D CNT micro-preconcentrator model as shown in Fig. 1 because of the large number of CNT bundles and the limited calculation capability of the computer. Therefore, the model was simplified to two dimensions, and we only considered one or two CNT forest patterns in the model. The speed of the input gas flow was set to 1 m/s to mimic the speed of human breath exhalation, and gas was flowed into each simulation model for 0.1 s from the left in the horizontal direction. The output pressure was set to 0 Pa, and N_2 gas was used as the carrier gas in the simulation. To evaluate the adsorption capability, 5000 particles were flowed in the carrier gas, and the number of particles reaching the CNT bundles was counted for each model. When the speed of a particle became less than 1.5×10^{-8} m/s near the CNT bundle surface, then we judged that the particle had been adsorbed.

The simplified 2D simulation models and the simulation results are summarized in Fig. 3. As shown in Fig. 3, we investigated six models (A–F). Model F showed the greatest adsorption capability because the largest number of particles reached the CNT bundles. The simulated speed distribution for each model is also presented by color differences. Note that a flow exists even inside the flower-leaf-shaped pattern, which is completely different from the case of a solid Si microstructure model, as shown in the inset of Fig. 3. The simulation result regarding the existence of a flow inside the CNT forest coincides with that of another study.[20]

The adsorption capability depends on the number of CNT forests and the interaction between the gas flow and the CNT forests. The difference in the adsorption capability between models A and B in Fig. 3 is caused by the difference in the contact area between the flowing gas molecules and the CNT forests. The adsorption capability differences between the models with one flower-leaf-shaped CNT forest (models A and B) and those with two flower-leaf-shaped CNT forests (models C–F) originated from the different number of CNT forests. For models C–F, the adsorption capability differences can be understood from the contact area differences and also the gas flow. In other words, models C and D showed lower adsorption capability than models E and F because of their smaller contact area with the gas flow. Moreover, because the gas flow is trapped between the two CNT forest structures in models D and F, models D and F showed greater adsorption capability than models C and E, respectively.

We also confirmed the height effect of the CNT bundles using a modified simulation model having three heights of 25, 50, and 100 μm. The higher the CNT bundle, the greater the number of adsorbed particles, as expected. To compare the adsorption capability of the CNT-based models with that of the Si microstructure models, simulation models A–F in Fig. 3 were

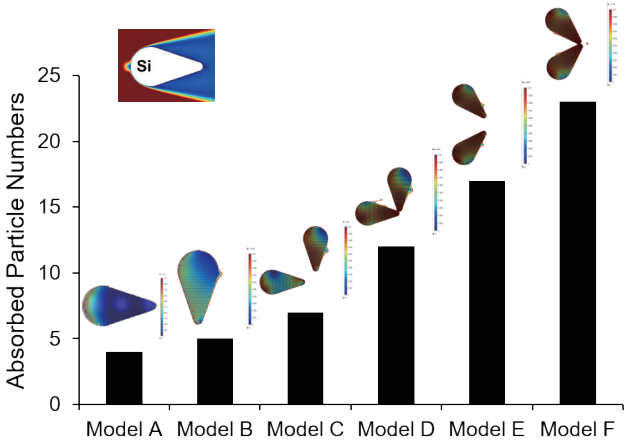

Fig. 3. (Color online) Simulation models and simulation results. The flow speed distribution is represented by color differences. Model F showed the greatest particle adsorption capability among the investigated models. The inset shows the flow speed distribution around Si-based model A. Note that the size of the flower leaf shape is the same for each model.

modified to a solid structure and the simulations with the same conditions were conducted. As a result, for models B–D, no particles reached the Si microstructure surfaces. For models A, E, and F, the number of particles reaching the Si microstructure surface was only 1/23 to 1/4 of that for the CNT forest models.

3. Fabrication of CNT-based Micro-preconcentrator

We fabricated a CNT-based micro-preconcentrator to verify its adsorption capability. The CNT forest pattern and its array were designed on the basis of the simulation results. In this section, we present the fabrication process of the CNT-based micro-preconcentrator and the results of fabrication.

The fabrication process of the CNT-based micro-preconcentrator is illustrated in Fig. 4. To grow CNTs on a 2 × 2 cm^2 Si substrate, we patterned a photoresist for the liftoff process, and a 10-nm-thick Al_2O_3 barrier layer and a 1-nm-thick Fe catalyst layer were sputtered [Fig. 4(a)]. Then, CNT forests were grown by heat filament chemical vapor deposition (CVD) after annealing the substrate at 650 °C. The reaction gases used for CNT growth were C_2H_2 and H_2. During the growth, the substrate temperature was 600 °C, and −300 V bias was applied to the substrate [Fig. 4(b)]. After the CNT growth, a glass substrate with an inlet and outlet can be anodically bonded as a lid if necessary [Fig. 4(c)].

We designed the CNT forest patterns on the basis of simulation models C–F shown in Fig. 3. In other words, the CNT forest patterns were designed in the shape of the flower leaf. Models C–F each became half of a single flower leaf shape. Moreover, regular and staggered arrays were considered as the array of the flower leaf pattern. The CNT forests were grown over an area of 1.5 × 1.3 mm^2 on the 2 × 2 cm^2 Si chip. Among the designed CNT forest patterns, we could only confirm the growth for the patterns based on models C, E, and F. However, micro-preconcentrators based on models E and F could not be used in a gas adsorption experiment

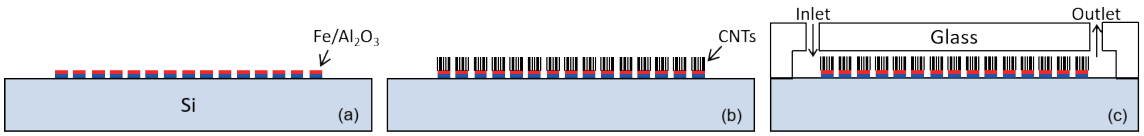

Fig. 4. (Color online) Fabrication process of the CNT-based micro-preconcentrator: (a) formation of Al_2O_3 barrier layer and Fe catalyst layer, (b) growth of CNT forests, and (c) bonding of glass substrate as a lid.

because the CNTs were not grown uniformly; on parts of the chip, the CNT forest patterns were not obvious or the height of the CNTs was low. On the other hand, in the case of the micro-preconcentrator having the regular array of a flower leaf shape designed on the basis of model C, although the CNT bundles were not vertically grown, we judged that the micro-preconcentrator could be used for the gas adsorption experiment. Moreover, the typical CNT height was approximately 70 μm. Figure 5 shows the micro-preconcentrator having the CNT forest pattern based on model C used in the gas adsorption experiment, which consists of multiwalled CNTs with an open end.

4. VOC Gas Adsorption Experiment and Discussion

We performed a trace-level gas adsorption experiment using the micro-preconcentrator shown in Fig. 5 to verify its gas preconcentration capability. In the experiment, three main steps were necessary: first, a trace-level gas was adsorbed on the micro-preconcentrator; second, the adsorbed gas was desorbed; third, the desorbed gas was introduced into equipment to analyze the gas components.

In the first step, we used a 1 ppb sample gas (Sumitomo Seika Chemicals Co., Ltd., Osaka, Japan) as the gas for the adsorption experiment. In the sample gas, three different VOC gases, pentane (C_5H_{12}), octane (C_8H_{18}), and undecane ($C_{11}H_{24}$), each with a concentration of 1 ppb, were mixed together. To adsorb the sample gases, the micro-preconcentrator was set in a laboratory-built apparatus that was made of stainless steel and provided two tubes for gas inflow and outflow. A photograph and schematic illustration of the apparatus are shown in Fig. 6. In fact, this apparatus plays a similar role to the lid shown in Fig. 4(c). The 1 ppb mixed VOC sample gases were introduced through the inlet shown in Fig. 6 into the micro-preconcentrator at a rate of 30 mL/min for 5 min for adsorption.

The second step was the desorption of the adsorbed gases. The adsorption force between the VOC gas molecules and the CNT surfaces is the van der Waals force. Therefore, desorption is easily achieved by applying thermal energy. In the experiment, we heated the apparatus containing the micro-preconcentrator with a ribbon heater at 300 °C for a sufficient time (typically 1 h). During the desorption process, both the inlet and outlet valves were closed and the desorbed gases were kept inside the apparatus.

In the final step, the outlet valve of the apparatus was opened and the desorbed gases were introduced into equipment for gas component analysis. In the experiment, we used gas chromatography for gas component analysis. The flame ionization detector (FID) of the gas chromatography equipment was used to analyze the gas compounds, and N_2 gas was used as the carrier gas.

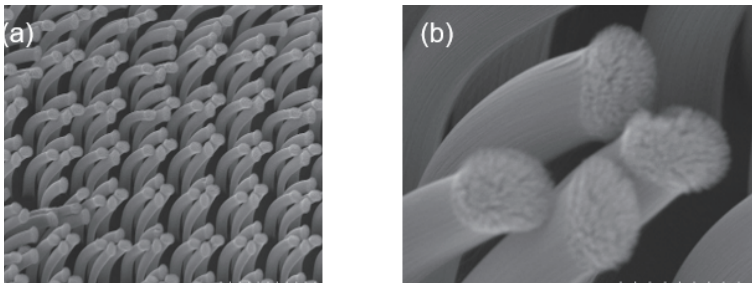

Fig. 5. SEM images of fabricated CNT-based micro-preconcentrator: (a) CNT forests and (b) magnification of four CNT bundles. The CNT forest pattern is based on model C (Fig. 3) and the array of CNT forests is regular.

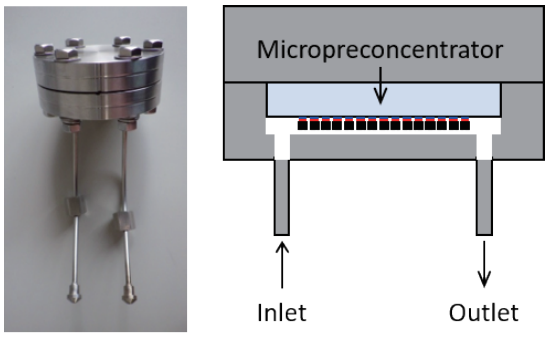

Fig. 6. (Color online) Photograph and schematic diagram of apparatus used to connect the micro-preconcentrator and the equipment for gas component analysis.

We clearly achieved the detection of 1 ppb VOC sample gases as shown in Fig. 7. FID output voltages were detected at 4.3–4.4, 8.3–8.4, and 10.8–11 min, corresponding to pentane, octane, and undecane, respectively. Note that the detectable minimum gas concentration of the FID is 1 ppm. This means that the CNT-based micro-preconcentrator achieved at least 1000-fold preconcentration. It is difficult to directly compare the preconcentration capability of the CNT-based micro-preconcentrator with that of the Si-based micro-preconcentrator, because the fabricated micro-preconcentrator models were different. When we used the CNT-based micro-preconcentrator shown in Fig. 5, the areas of the FID detection peaks in Fig. 7 were 2.1 to 2.6 times larger than those when the typical Si-based micro-preconcentrator was used. In other words, the amounts of detected gases, which represent the preconcentration capability of the CNT-based micro-preconcentrator, were 2.1 to 2.6 times larger than those of the Si-based micro-preconcentrator. Moreover, in the case of the CNT-based micro-preconcentrator, the FID peak values, representing the sensitivity, ranged from approximately the same as those for the Si-based micro-preconcentrator to approximately twice as large. The preconcentration capability of the Si-based micro-preconcentrator will be discussed in detail in a separate paper.

As a result of the adsorption experiment, we found that the CNT-based micro-preconcentrator is a promising device for detecting trace-level VOC biomarkers contained in exhaled breath. Furthermore, CNT forests have the advantage that their entire surface can adsorb VOCs. In the case of the Si microstructure, it is necessary to use a coating material called TENAX-TA to

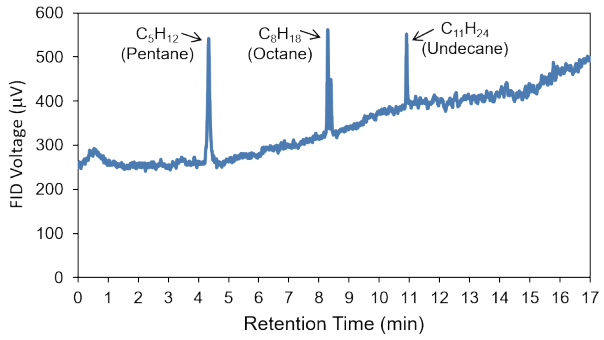

Fig. 7. (Color online) Flame ionization detector voltage plotted against retention times: three different sample gases, each with a concentration of 1 ppb, were detected using conventional gas chromatography.

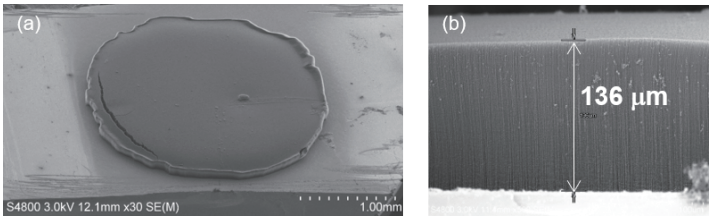

Fig. 8. (a) and (b) SEM images of CNT forest grown by thermal CVD: the diameter of the CNT forest is 3 mm and the height of the CNT forest is 136 μm.

adsorb VOC gases. Therefore, the adsorption capability of the Si-based micro-preconcentrator depends on the coating condition of the TENAX-TA. However, there is also a problem to be solved in the case of the CNT-based micro-preconcentrator to ensure stable performance. To obtain CNT-based micro-preconcentrators with consistent performance, the growth orientation and height of the CNT forests should be controlled. Currently, we are studying the optimization of the CNT forest growth conditions to obtain a vertically grown and height-controlled CNT forest. The CNT growth method used in this study is thermal CVD, which is the simplest CNT growth method and has the fewest growth parameters. The most dominant growth condition in thermal CVD is the growth temperature. Using the laboratory-built thermal CVD equipment, we obtained vertically grown multiwalled CNTs with an open end whose heights were more than 100 μm. A typical CNT forest grown in this study is shown in Fig. 8. Before the growth, a 10-nm-thick sputtered Al_2O_3 barrier layer and a 1-nm-thick vacuum-evaporated Fe catalyst layer were deposited. The diameter of the CNT forest pattern was 3 mm and the height of the grown CNT forest was 136 μm as shown in Figs. 8(a) and 8(b), respectively. The growth temperature was 750 °C, and the CNTs grew perpendicularly to the substrate. Higher preconcentration capability is expected if the flower-leaf-shaped CNT forest grown by thermal CVD is applied to the micro-preconcentrator.

5. Conclusions

In this study, we proposed a breath analysis scheme for the diagnosis of human or canine cancer, in which a micro-preconcentrator is used for the preconcentration of trace-level biomarkers contained in exhaled breath, and conventional gas analysis equipment, such as gas chromatography and gas mass chromatography equipment, is used for the detection of biomarkers. This diagnosis scheme based on breath analysis is suitable for early cancer diagnosis and can also respond to diverse VOC biomarkers.

We developed a handheld CNT-based micro-preconcentrator that consists of CNT forests. The CNT forest pattern and its array were designed by performing a quantitative simulation study. As a result, we found that a flower-leaf-shaped CNT forest pattern maximized the contact area between the breath flow and the CNT forest surface. We fabricated a CNT-based micro-preconcentrator and evaluated its performance, where the CNT forest was grown by heat filament CVD. Although the grown CNT bundles were not vertical and their height could not be controlled, we successfully obtained a micro-preconcentrator that could be evaluated. In the evaluation experiment, first we adsorbed 1 ppb mixed VOC sample gases on a CNT-based micro-preconcentrator. Then, the absorbed sample gases were desorbed by heating, and the desorbed gas compounds were analyzed using conventional gas chromatography. As a result, we achieved ppb-level gas detection using gas chromatography, whose minimum detectable concentration of a sample gas is 1 ppm order, thus demonstrating that the developed CNT-based micro-preconcentrator has at least 1000-fold preconcentration capability. Therefore, we expect that the CNT-based micro-preconcentrator can be used as a key device in early cancer diagnosis based on breath analysis.

However, there are some problems that need to be solved. One of them is the fabrication of a CNT-based micro-preconcentrator with consistent performance. To obtain vertically grown and height-controlled CNT forests, we are studying the optimization of CNT growth by thermal CVD. Demonstration of the preconcentration capability of the micro-preconcentrator consisting of a CNT forest grown by thermal CVD is planned in the near future. Moreover, cancer biomarkers must be defined for dogs, which we are currently examining in a research project. Finally, to reduce the time for gas desorption, we plan to improve the apparatus shown in Fig. 6 by installing a heater inside the apparatus.

Acknowledgments

The authors would like to thank Prof. Takahito Ono of Tohoku University and Dr. Hidetoshi Miyashita of Sony Semiconductor Manufacturing Corporation for their support in the CNT growth by heat filament CVD.

References

1 H. Nagai and Y. H. Kim: J. Thorac. Dis. **9** (2017) 448. https://doi.org/10.21037/jtd.2017.02.75
2 F. B. Ahmad and R. N. Anderson: JAMA **325** (2021) 1829. https://doi.org/10.1001/jama.2021.5469
3 S. Tsugane: Eur. J. Clin. Nutr. **75** (2021) 921. https://doi.org/10.1038/s41430-020-0677-5

4 A. Soni, K. Simon, J. Cawley, and L. Sabik: Am. J. Public Health **108** (2018) 216. https://doi.org/10.2105/AJPH.2017.304166
5 J. Jiang, H. Zhao, W. Shu, J. Tian, Y. Huang, Y. Song, R. Wang, E. Li, D. Slamon, D. Hou, X. Du, L. Zhang, Y. Chen, and Q. Wang: Sci. Rep. **7** (2017) 42612. https://doi.org/10.1038/srep42612
6 S. Wan, T. H. Kim, K. J. Smith, R. Delaney, G.-S. Park, H. Guo, E. Lin, T. Plegue, N. Kuo, J. Steffes, C. Leu, D. M. Simeone, N. Razimulava, N. D. Parikh, S. Nagrath, and T. H. Welling: Sci. Rep. **9** (2019) 18575. https://doi.org/10.1038/s41598-019-54960-y
7 Saliva Tech K.K.: https://www.salivatech.co.jp (in Japanese) (accessed March 2022).
8 A. Asai, M. Konno, M. Ozaki, K. Kawamoto, R. Chijimatsu, N. Kondo, T. Hirotsu, and H. Ishii: Oncotarget **12** (2021) 1687. https://doi.org/10.18632/oncotarget.28035
9 M. Phillips, R. N. Cataneo, C. Saunders, P. Hope, P. Schmitt, and J. Wai: J. Breath Res. **4** (2010) 026003. https://doi.org/10.1088/1752-7155/4/2/026003
10 M. Phillips, R. N. Cataneo, A. R. Cummin, A. J. Gagliardi, K. Gleeson, J. Greenberg, R. A. Maxfield, and W. N. Rom: Chest **123** (2003) 2115. https://doi.org/10.1378/chest.123.6.2115.
11 S. R. Markar, T. Wiggins, S. Antonowicz, S.-T. Chin, A. Romano, K. Nikolic, B. Evans, D. Cunningham, M. Mughal, J. Lagergren, and G. B. Hanna: JAMA Oncol. **4** (2018) 970. https://doi.org/10.1001/jamaoncol.2018.0991
12 G. Peng, M. Hakim, Y. Broza, S. Billan, R. Abdah-Bortnyak, A. Kuten, U. Tisch, and H. Haick: Br. J. Cancer **103** (2010) 542. https://doi.org/10.1038/sj.bjc.6605810
13 C. Wang, C. Ke, X. Wang, C. Chi, L. Guo, S. Luo, Z. Guo, G. Xu, F. Zhang, and E. Li: Anal. Bioanal. Chem. **406** (2014) 4757. https://doi.org/10.1007/s00216-014-7865-x
14 M. Phillips, R. N. Cataneo, J. A. Cruz-Ramos, J. Huston, O. Ornelas, N. Pappas, and S. Pathak: Breast Cancer Res. Treat. **170** (2018) 343. https://doi.org/10.1007/s10549-018-4764-4
15 W. Shin, T. Itoh, and N. Izu: Synthesiology **8** (2016) 211.
16 G. Yoshikawa, T. Akiyama, S. Gautsch, P. Vettiger, and H. Rohrer: Nano Lett. **11** (2011) 1044. https://doi.org/10.1021/nl103901a
17 The Engineering News: https://www.theengineer.co.uk/content/news/gas-sensor-device-can-predict-asthma-attacks (written by J. Ford in Feb. 9, 2011) (accessed March 2022).
18 B. Alfeeli and M. Agah: IEEE Sensors J. **11** (2011) 2756. https://doi.org/10.1109/JSEN.2011.2160390
19 N. Kakita, H. Miyashita, S. Kishida, J.-O. Lee, and S.-S. Lee: Proc. IEEE Sensors Conf. (2013) 1. https://doi.org/10.1109/ICSENS.2013.6688334
20 G. D. Chen, F. Fachim, M. Fernandez-Suarez, B. L. Wardle, and M. Toner: Small **7** (2011) 1061. https://doi.org/10.1002/smll.201002076

About the Authors

Keiji Nakamoto received his B.E. and M.E. degrees from Tottori University, Japan, in 2018 and 2020, respectively. Since 2020, he has been studying for a Ph.D. degree at the Graduate School of Engineering, Tottori University while also working at Toshiba Tec Corporation as a research engineer. His research interests are in MEMS and nanotechnology. (D20T2003B@edu.tottori-u.ac.jp)

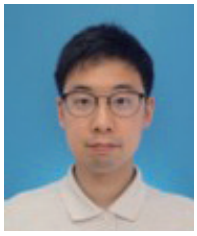

Tomoaki Kageyama received his B.E. degree from the Faculty of Engineering, Tottori University, Japan, in 2014 and his M.E. and Ph.D. degrees from the Graduate School of Engineering, Tottori University in 2016 and 2019, respectively. Since 2021, he has been an assistant professor at Tottori University. His research interests are in MEMS, sensors, sensor networks, and IoT systems. (tkageyama@tottori-u.ac.jp)

Shunsaku Hosoi received his B.E. degree from Tottori University, Japan, in 2021. Since 2021, he has been studying for a master's degree at the Graduate School of Engineering, Tottori University. His research interests are in nanotechnology, including carbon nanotube fabrication and its applications. (M21J4052B@edu.tottori-u.ac.jp)

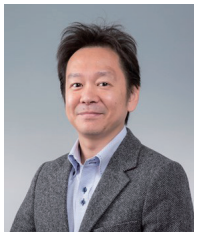

Tadao Matsunaga received his B.E. degree from the Faculty of Science and Engineering, Saga University in 1994 and worked at Akebono Brake Industries from 1994 to 2002. He received his Ph.D. degree in engineering from Tohoku University in 2002. From 2003 to 2004, he was at the Japan Science and Technology Agency (JST). From 2004 to 2016, he was an assistant professor, and from 2017 to 2018, an associate professor at Tohoku University. Since 2019, he has been an associate professor at Tottori University.
(matsunaga@tottori-u.ac.jp)

Sang-Seok Lee received his Ph.D. degree from Tohoku University, Japan, in 1998. In 1999, he was a post-doctorate researcher at Tohoku University. From 2000 to 2001, he was a post-doctorate researcher at Delft University of Technology, Netherlands. From 2002 to 2011, he was a researcher at Mitsubishi Electric Corporation, Japan. Since 2011, he has been a professor at Tottori University, Japan. His research interests are in MEMS, metamaterials, and sensors. (sslee@tottori-u.ac.jp)